

Low-Cost Gel Polymer Electrolyte for High-Performance Aluminum-Ion Batteries

Zhidong Liu, Xiaohang Wang, Zhiyuan Liu, Shuqing Zhang, Zichuan Lv, Yanyan Cui, Li Du, Kaiming Li, Guoxin Zhang, Meng-Chang Lin, and Huiping Du*

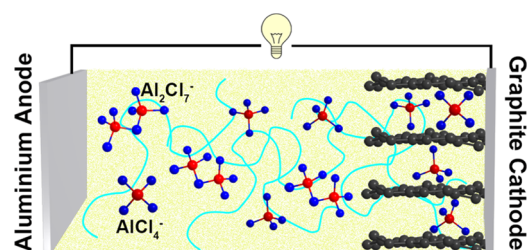
ABSTRACT: The classical AlCl_3 /imidazole chloride salt ionic liquid electrolytes are expensive, corrosive, and environmentally sensitive, which limit the large scale application of aluminum ion batteries. Herein, a gel polymer electrolyte is prepared through a facile process using a low cost AlCl_3 / Et_3NHCl ionic liquid as the plasticizer and polyamide as the polymer matrix. The gel polymer electrolyte achieves a decent ionic conductivity of $3.86 \times 10^{-3} \text{ S cm}^{-1}$, a wide electrochemical stability window of 2.6 V (vs Al), and long term interfacial stability at room temperature. The assembled Al//graphite battery delivers considerable rate capability and excellent cycling performance. Besides, the gel polymer electrolyte can alleviate both moisture sensitivity and leakage corrosion issues owing to the full encapsulation of the ionic liquid by polyamide polymeric matrix. The gel polymer electrolyte should offer great potential for aluminum ion battery applications.

KEYWORDS: aluminum ion batteries, leakage corrosion, moisture sensitivity, low cost, gel polymer electrolyte, polyamide

1. INTRODUCTION

Low cost, high safety, and long life are key factors for grid scale energy storage to make use of clean, sustainable energy.^{1–6} Rechargeable aluminum ion batteries that consist of an aluminum metal anode, an ionic liquid electrolyte, and a graphite cathode can sustain for thousands of cycles and exhibit low flammability.^{7–11} In addition, both aluminum and graphite are abundant in nature and highly tolerant toward oxygen and moisture.^{12–15} However, the classical ionic liquid electrolytes (mixing AlCl_3 with imidazole chloride salts that bear different alkyl side chains, i.e., 1 ethyl 3 methylimidazolium chloride (EMIC) and 1 butyl 3 methylimidazolium chloride (BMIC)) are expensive, corrosive, and moisture sensitive, which severely limit the grid scale application of aluminum ion batteries.^{8,12,16,17}

Some studies have shown that AlCl_3 /urea deep eutectic solvent, which is less expensive than AlCl_3 /EMIC ionic liquid, could also work in Al//graphite batteries.^{18–21} Yet, a specific cathode capacity of $\approx 73 \text{ mAh g}^{-1}$ was obtained accompanied by only ~ 200 cycles at room temperature.¹⁸ When the temperature was increased to $120 \text{ }^\circ\text{C}$, the capacity can be improved to about 94 mAh g^{-1} but only 75 mAh g^{-1} remained after 500 cycles.²² A low cost $\text{NaCl}-\text{AlCl}_3$ molten salt was also proposed to assemble Al//graphite batteries, which displayed capacities of 60 and 43 mAh g^{-1} after 5000 and 9000 cycles, respectively.²³ Nevertheless, the inorganic molten salts usually have a relatively high melting point, causing the operation temperature of aluminum ion batteries to be above $80 \text{ }^\circ\text{C}$.^{24–26} Triethylamine hydrochloride (Et_3NHCl) salt is an industrial



waste, which is abundant, intractable, and cheap. Recently, AlCl_3 / Et_3NHCl room temperature ionic liquid was synthesized by mixing AlCl_3 with Et_3NHCl and used as an electrolyte of Al//graphene battery. The battery shows a cathodic capacity of 112 mAh g^{-1} after 30 000 cycles with 97.3% retention at the current density of 5 A g^{-1} and maintains a high capacity of $\sim 90 \text{ mAh g}^{-1}$ even at an ultrahigh current density of 18 A g^{-1} .²⁷ Despite the low cost and high ionic conductivity, the AlCl_3 / Et_3NHCl ionic liquid electrolyte is still corrosive and moisture sensitive. A new AlCl_3 /4 ethylpyridine ionic liquid electrolyte free of Al_2Cl_7^- was proposed for Al//graphite batteries, which showed lower corrosivity toward Al, Cu, and Ni electrodes compared with AlCl_3 /EMIC ionic liquid and displayed moisture insensitive behavior. Yet, a capacity of 30 mAh g^{-1} remains when the current density is changed from 25 mA g^{-1} (95 mAh g^{-1}) to 300 mA g^{-1} .¹²

Dai and co workers prepared a gel polymer electrolyte with an AlCl_3 complexed acrylamide as a functional monomer and AlCl_3 /EMIC ionic liquid as a plasticizer via free radical polymerization in volatile dichloromethane. The gel polymer electrolyte still showed reversible aluminum deposition/stripping behavior even after being exposed to air for 10

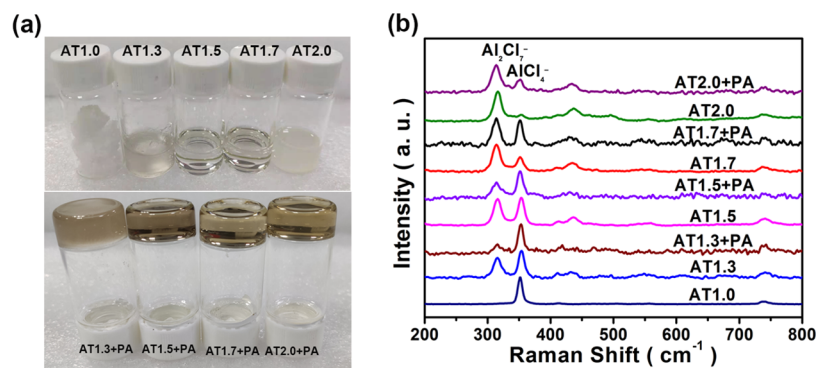


Figure 1. (a) Digital photos of the AlCl₃/Et₃NHCl ($r = 1.0, 1.3, 1.5, 1.7, 2.0$) mixtures and the corresponding gel polymer electrolytes. (b) Raman spectra of the AlCl₃/Et₃NHCl ($r = 1.0, 1.3, 1.5, 1.7, 2.0$) mixtures and the corresponding gel polymer electrolytes.

min, suggesting the alleviation of moisture sensitivity.²⁸ Subsequently, Jiao and co workers employed the gel polymer electrolyte to assemble Al//graphite batteries, which displayed an impressive capacity of $\approx 120 \text{ mAh g}^{-1}$ with good cycling stability beyond 100 cycles and high Coulombic efficiency of $>90\%$ at the current density of 60 mA g^{-1} .²⁹ They also prepared a polyacrylamide based gel polymer electrolyte with AlCl₃/Et₃NHCl ionic liquid as the plasticizer via free radical polymerization, and the assembled Al//graphite batteries displayed a capacity of 90 mAh g^{-1} after 800 cycles with a Coulombic efficiency of 95% under a high current density.³⁰ Note that the gel polymer electrolyte could substantially suppress the gas production, prevent unexpected volume expansion, and avoid leakage corrosion issues compared to ionic liquid electrolytes, resulting in high Coulombic efficiency and high cycling stability.^{29,30}

Herein, we developed a novel gel polymer electrolyte by combining polyamide (PA) with the low cost AlCl₃/Et₃NHCl ionic liquid (IL) via a simple procedure. Adding PA into the acidic AlCl₃/Et₃NHCl IL through stirring and heating, we prepared the PA based gel polymer electrolyte after cooling. The preparation process of this gel polymer electrolyte is simple, sustainable, and environmentally friendly due to no use of organic solvent. The assembled Al//graphite battery maintains a discharge capacity of 94.6 mAh g^{-1} and high Coulombic efficiency of $>99.2\%$ over 2000 cycles at the current density of 200 mA g^{-1} . As AlCl₃/Et₃NHCl IL is encapsulated by the PA matrix, the PA based gel polymer electrolyte presents a solid like state and exhibits alleviated moisture sensitivity and leakage corrosion.

2. EXPERIMENTAL SECTION

2.1. Preparation of the Ionic Liquid Electrolyte. At room temperature, certain moles of anhydrous AlCl₃ were slowly added into Et₃NHCl with vigorous magnetic stirring for 6 h to obtain the needed ionic liquids (AlCl₃/Et₃NHCl, $r = 1.0, 1.3, 1.5, 1.7, 2.0$) in an argon filled glovebox.

2.2. Preparation of the Gel Polymer Electrolytes. To prepare the gel polymer electrolytes, the mixtures comprised of an amount of polyamide and the above ionic liquids (AlCl₃/Et₃NHCl, $r = 1.3, 1.5, 1.7, 2.0$) were heated ($60 \text{ }^\circ\text{C}$) under stirring conditions for 8 h. The mass ratio of polyamide and ionic liquids is 1:20.

2.3. Preparation of the Graphite Cathode and Assembly of the Quasi-Solid-State Al//Graphite Battery. To obtain the graphite cathode, the homogeneous graphite slurry containing 95 wt % SP 1 graphite powder and 5 wt % LA132 was coated on a Ni foil current collector and dried at $120 \text{ }^\circ\text{C}$ under vacuum for 12 h. The loading of graphite is $\sim 2 \text{ mg cm}^{-2}$. The Al//graphite batteries were

assembled into coin cells or pouch cells as needed. The sandwich structure of the batteries consisted of an Al foil anode, a gel polymer electrolyte coated on the glass fiber separator, and a graphite cathode.

2.4. Electrochemical and Physical Measurements. The Raman spectra were collected on a Thermo Fisher Scientific Raman spectrometer (DXR2) using a 532 nm laser. The charging/discharging test for the Al//graphite batteries was conducted on a Land BT2000 battery test system (Wuhan, China) from 1.0 to 2.45 V. Linear sweep voltammetry (LSV) of the Al//gel polymer electrolyte//Mo was recorded on VMP 3 with a sweep rate of 1.0 mV s^{-1} . The ionic conductivity was calculated at different temperatures ranging from room temperature to $80 \text{ }^\circ\text{C}$ by means of electrochemical impedance spectroscopy (EIS) analysis. The gel polymer electrolyte was sandwiched between two Mo foil electrodes and the spectra were recorded in the frequency range from 100 mHz to 1 MHz with an AC amplitude of 5 mV. The interfacial stability of the gel polymer electrolyte was evaluated by a galvanostatic charge/discharge test at the current density of 0.1 mA cm^{-2} for each 1 h. In situ X ray diffraction (XRD) pattern was recorded in the D8 Advance X ray powder diffraction apparatus. In situ Raman pattern was examined in a DXR2 Raman spectrometer.

3. RESULTS AND DISCUSSION

Table S1 lists the specific numerical costs of AlCl₃, EMIC, and Et₃NHCl, which suggests that the AlCl₃/Et₃NHCl system has low cost compared to the AlCl₃/EMIC system. To comprehensively study the AlCl₃/Et₃NHCl system, AlCl₃/Et₃NHCl mixtures with different molar ratios were prepared as shown at the top of Figure 1a. When the molar ratio of AlCl₃/Et₃NHCl is 1, the mixture (AT1.0) is solid. When the molar ratios of AlCl₃/Et₃NHCl are 1.3, 1.5, 1.7, or 2.0, the mixtures (AT1.3, AT1.5, AT1.7, and AT2.0) are liquid. However, when the molar ratio of AlCl₃/Et₃NHCl is 1.3, the formed liquid (AT1.3) is not stable, fluctuating between liquid state (Figure S1a) and transparent ice like state (Figure S1b); when the mole ratio of AlCl₃/Et₃NHCl is 2.0, part AlCl₃ could not be dissolved and the AlCl₃/Et₃NHCl liquid is cloudy. The corresponding AlCl₃/Et₃NHCl ($r = 1.5, 1.7, 2.0$) gel polymer electrolytes (AT1.5 + PA, AT1.7 + PA, AT2.0 + PA) are transparent brown colloid while the AlCl₃/Et₃NHCl ($r = 1.3$) gel polymer electrolyte (AT1.3 + PA) is more of a solid state than a colloidal state (the bottom of Figure 1a). Figure 1b gives the Raman spectra of different molar ratios of AlCl₃/Et₃NHCl mixtures and the corresponding gel polymer electrolytes. The peaks at around 310 and 350 cm^{-1} can be assigned to Al₂Cl₇⁻ and AlCl₄⁻ anions, respectively. The Raman peak intensity ratios of 310 and 350 cm^{-1} can be used to evaluate the content ratio of Al₂Cl₇⁻ and AlCl₄⁻ anions.^{19,20,27,31} It can be observed that the content ratio of

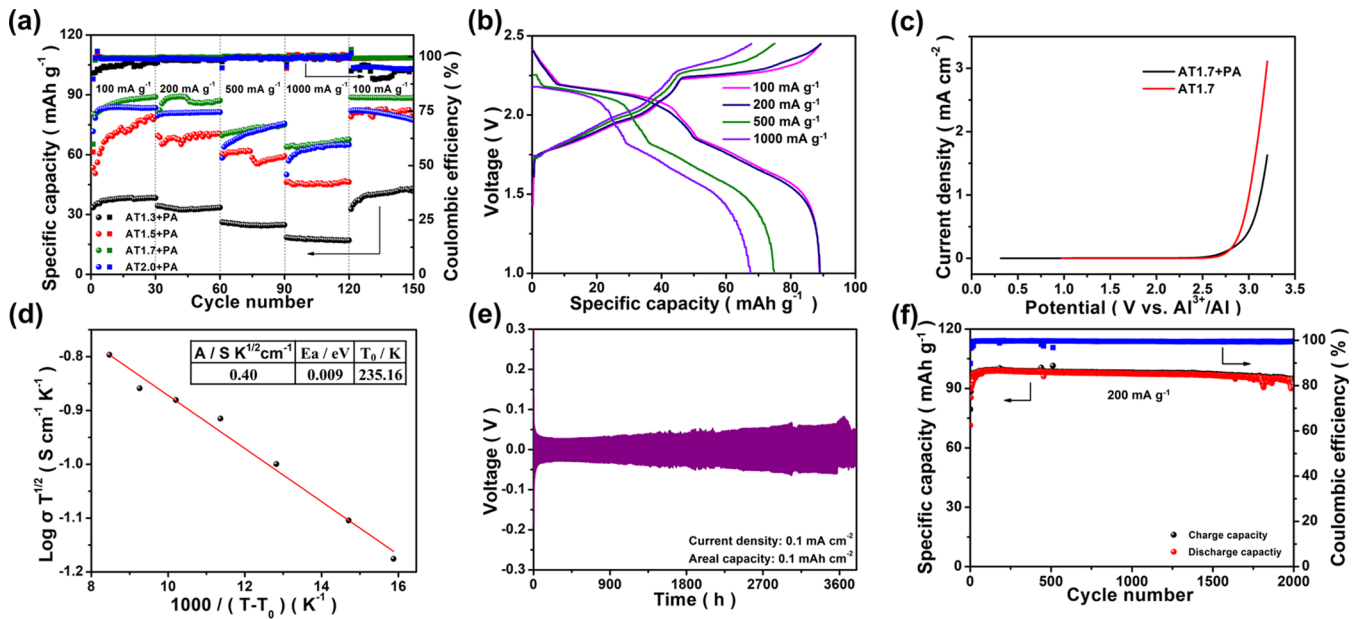


Figure 2. (a) Rate capabilities of the assembled Al//graphite batteries using various AlCl₃/Et₃NHCl ($r = 1.3, 1.5, 1.7, 2.0$) gel polymer electrolytes. (b) Charge–discharge profiles of the Al//graphite battery with the AlCl₃/Et₃NHCl ($r = 1.7$) gel polymer electrolyte at different current densities. (c) LSV curves of the AlCl₃/Et₃NHCl ($r = 1.7$) ionic liquid electrolyte and the AlCl₃/Et₃NHCl ($r = 1.7$) gel polymer electrolyte. (d) Temperature dependent ionic conductivity of AlCl₃/Et₃NHCl ($r = 1.7$) gel polymer electrolyte. (e) Galvanostatic cycling behavior of symmetric Al//Al cell using AlCl₃/Et₃NHCl ($r = 1.7$) gel polymer electrolyte at the current density of 0.1 mA cm⁻². (f) Cycling performance of the Al//graphite battery using AlCl₃/Et₃NHCl ($r = 1.7$) gel polymer electrolyte at room temperature.

Al₂Cl₇⁻/AlCl₄⁻ increases with the molar ratio of AlCl₃/Et₃NHCl for AlCl₃/Et₃NHCl ($r = 1.3, 1.5, 1.7, 2.0$) mixtures, which is because AlCl₄⁻ and AlCl₃ would be transformed into Al₂Cl₇⁻.^{20,27,31,32} It is the same trend for the AlCl₃/Et₃NHCl ($r = 1.3, 1.5, 1.7, 2.0$) gel polymer electrolytes. It is also noted that the content ratio of Al₂Cl₇⁻/AlCl₄⁻ decreases when PA is added into the AlCl₃/Et₃NHCl mixtures. As shown in Figure S2, the band at 1647 cm⁻¹ corresponding to Amide I of PA is red shifted to 1633 cm⁻¹ in AT1.7 + PA. The N–H stretching frequency is shifted from 3302 cm⁻¹ in PA to 3353 cm⁻¹ in AT1.7 + PA. The band at 1542 cm⁻¹ is attributed to the α and β crystalline phases that belong to the unassociated amide in PA, which is shifted to 1557 cm⁻¹ in AT1.7 + PA. The bands at 930 cm⁻¹ and 1120 cm⁻¹ correspond to the C–CO stretching in the crystalline α and β phases and in the amorphous phase, respectively, which are shifted to 942 and 1113 cm⁻¹ separately. The above shift suggests that PA coordinates with Lewis acid (AlCl₃),^{33–36} so Al₂Cl₇⁻ decreases in the gel polymer electrolyte. All of the AlCl₃/Et₃NHCl ($r = 1.3, 1.5, 1.7, 2.0$) gel polymer electrolytes can be used in rechargeable aluminum ion batteries due to the coexistence of electrochemically active anions of Al₂Cl₇⁻ and AlCl₄⁻. Figure S3 shows that Al can strip/plat reversibly in the AlCl₃/Et₃NHCl ($r = 1.7$) gel polymer. After being exposed in the air for 10 min, reversible Al deposition/stripping behavior is still observed for the AlCl₃/Et₃NHCl ($r = 1.7$) gel polymer electrolyte while the electrochemical activity is lost for the AlCl₃/Et₃NHCl ($r = 1.7$) ionic liquid electrolyte (Figure S4). The AlCl₃/Et₃NHCl ($r = 1.7$) gel polymer electrolyte exhibits mitigated moisture sensitivity compared to the AlCl₃/Et₃NHCl ($r = 1.7$) ionic liquid electrolyte, which would be beneficial for the Al//graphite battery assembly.

We assemble the Al//graphite batteries composed of Al anode and graphite cathode, separated by the AlCl₃/Et₃NHCl ($r = 1.3, 1.5, 1.7, 2.0$) gel polymer electrolytes, respectively. As

shown in Figure 2a, the Al//graphite batteries using the AlCl₃/Et₃NHCl ($r = 1.7$) gel polymer electrolyte exhibit the best rate performance, which achieve discharge capacities of 89.3, 89.1, 75.0, and 67.3 mAh g⁻¹ when the current densities are 100, 200, 500, and 1000 mA g⁻¹, respectively. Also, the specific capacity recovers to 88.7 mAh g⁻¹ when the current density is returned to 100 mA g⁻¹. At the same time, the Coulombic efficiency remains above 99.5%. Figure 2b shows the corresponding charge–discharge profiles, which display obvious charging and discharging platforms under different current densities. Due to the outstanding electrochemical performance of the AlCl₃/Et₃NHCl ($r = 1.7$) gel polymer electrolyte in the Al//graphite batteries, we performed a special study on the AlCl₃/Et₃NHCl ($r = 1.7$) gel polymer electrolyte (named as gel polymer electrolyte (GPE) here after). Figure 2c presents the LSV curves of the AlCl₃/Et₃NHCl ($r = 1.7$) IL and GPE. GPE has a similar electrochemical window (2.6 V vs Al) with AlCl₃/Et₃NHCl ($r = 1.7$) IL. Figure 2d shows that the ionic conductivity increases with temperature, conforming to the Vogel–Tammann–Fulcher (VTF) empirical equation: $\sigma = AT^{-1/2} \exp(-E_a/(R(T - T_0)))$, where A is the pre exponential factor, E_a is the activation energy, R is the ideal gas constant, and T_0 is a parameter related to the glass transition temperature.³² The fitting activation energy is $E_a = 0.009$ eV, suggesting that GPE possesses a low energy barrier of ion transfer. Table S2 shows the ionic conductivities of the gel polymer electrolyte at different temperatures. The ionic conductivity is up to 3.86×10^{-3} S cm⁻¹ at room temperature. Figure 2e shows the galvanostatic cycling behavior of the symmetric Al//GPE//Al cell at the current density of 0.1 mA cm⁻². The working time is more than 3800 h, suggesting that GPE possesses excellent interfacial stability.³⁷ The Al//graphite battery with GPE maintains a discharge capacity of 94.6 mAh g⁻¹ with less than 3% capacity decay and high

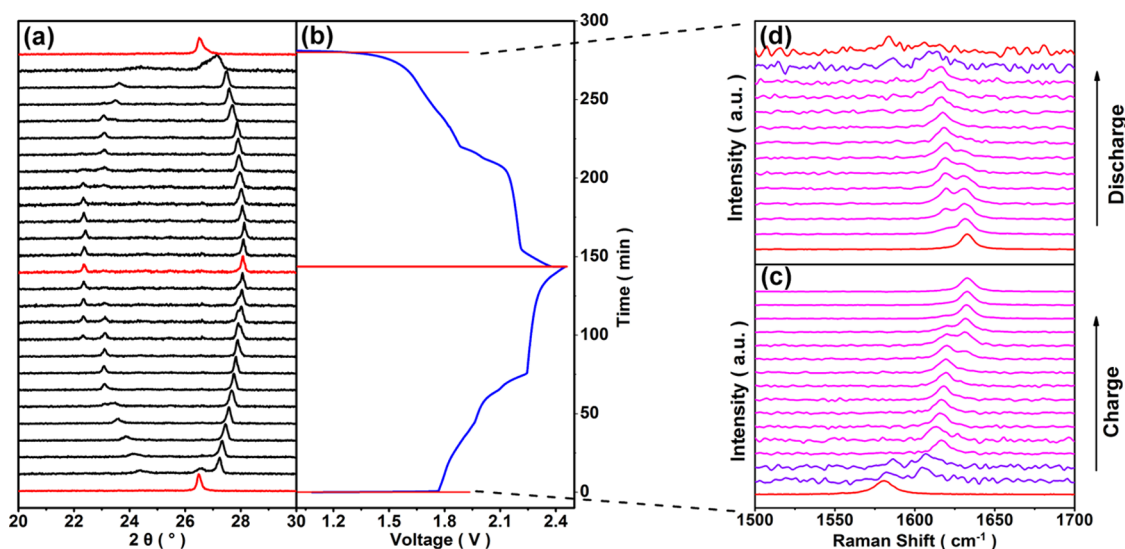


Figure 3. (a) In situ XRD spectra of the graphite cathode in the Al//GPE//graphite battery during the charging/discharging processes. (b) The corresponding charge–discharge profiles of the Al//GPE//graphite battery. (c) Operando Raman spectra recorded on the graphite cathode in the (c) charging and (d) discharging processes.

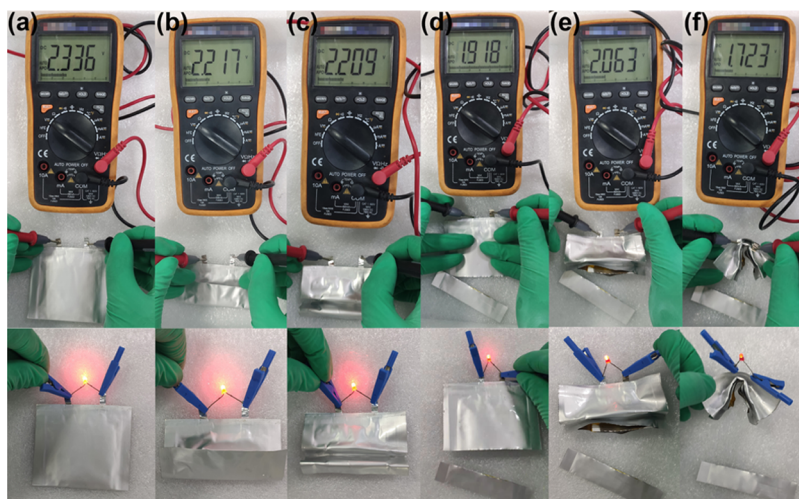


Figure 4. Illustration of the Al//GPE//graphite battery about voltage and powering for a LED lamp under various states: (a) origin, (b) bending, (c) two folds, (d) cut off, (e) cut off and two folds, and (f) cut off and three folds.

Coulombic efficiency of $>99.2\%$ over 2000 cycles at the current density of 200 mA g^{-1} (Figure 2f). As shown in Figure S5, the charge–discharge profiles at different cycles exhibit distinct voltage plateaus. Figures S6 and S7 show scanning electron microscopy (SEM) images of the graphite cathode and the Al foil anode before and after cycling. Pristine graphite is a bulk material stacked by multiple layers (Figure S6a,c). After cycling, the graphite layers become more uniform (Figure S6b,d). The surface of the Al foil anode is rough (Figure S7a,c) before cycling but becomes smooth after cycling with a small amount of corrosion and no dendrites (Figure S7b,d). This explains the excellent cycling performance of the Al//graphite batteries. The stable operation time is $\sim 1892 \text{ h}$, which is competitive compared to the previous reports (Table S3), indicating that GPE possesses long term stability.^{10,18–20,25,27,29,30,38–41} GPE can also inhibit the self discharge behavior of the Al//graphite battery effectively compared with the $\text{AlCl}_3/\text{Et}_3\text{NHCl}$ ($r = 1.7$) IL. Both the Al//GPE//graphite battery and the Al//IL//graphite battery are

charged to 2.45 V at the current density of 200 mA g^{-1} . Figure S8 shows variations of open circuit voltages of both Al//graphite batteries within 100 h rest, revealing that the open circuit voltages of the Al//GPE//graphite battery and the Al//IL//graphite battery are dropped to 2.15 and 1.84 V , respectively.

To understand the mechanism of the electrochemical energy storage in Al//graphite batteries with GPE, in situ X ray diffraction (XRD) and operando Raman spectroscopy are conducted during the charging/discharging process at a constant current density. The pristine graphite presents a sharp (002) peak at $2\theta = 26.5^\circ$ (the red line in the bottom of Figure 3a), corresponding to d spacing = 3.36 \AA . Upon charging, the (002) peak gradually disappears and two new peaks gradually appear at both sides of the (002) peak, indicating the formation of a graphite intercalated compound (GIC) by anion intercalation into the graphite layers.^{42,43} The corresponding charge–discharge profiles are shown in Figure 3b. As the charging process proceeds, three peaks appear with

the new peak at the left side of the (002) peak splitting into two peaks. When the voltage reaches 2.45 V, the two peaks fix at $2\theta = 28.1^\circ$ (d spacing = 3.17 Å) and 22.3° (d spacing = 3.98 Å) (the red line in the middle of Figure 3a). The change of the graphite peaks is reversed in the discharging process. The stage number (n) of the graphite intercalated compound (GIC) at a fully charged state can be calculated according to the following equation⁴⁴

$$n = 1/(\sin \theta_{(00n+2)}/\sin \theta_{(00n+1)} - 1) - 1$$

so, at a fully charged state, the graphite reaches stage 3 GIC.

Figure 3c,d records the operando Raman spectra of the graphite cathode during charging/discharging. When charging, the G band (1582 cm^{-1}) is split into two Raman modes of a lower frequency component E_{2g2i} (1586 cm^{-1}) and a higher frequency component E_{2g2b} (1609 cm^{-1}), which are associated with vibrations of carbon atoms in an intercalated graphite layers and in intercalated graphite layers, respectively (Figure 3c).^{41,45} At higher potentials, the E_{2g2b} peak is blue shifted and the E_{2g2i} peak disappears, evolving into a single, dominant peak at 1635 cm^{-1} at 2.45 V. The reversed spectral changes are observed in the discharge process, as shown in Figure 3d. According to previous reports,^{46,47} the peak positions of the G band are a function of the reciprocal stage index of GICs. Hence, the new peak at 1635 cm^{-1} is confirmed to be a stage 1 GIC. In contrast with XRD spectroscopy that detects the bulk, Raman spectroscopy collects surface information. Due to easier intercalation into graphite surface layers than into the graphite interior layers, a lower stage number result is obtained from Raman than that from XRD. From the above discussion, the energy storage/release in Al//graphite batteries with GPE are based on the reversible intercalation/deintercalation of chloroaluminate anions into/out of the graphite layers in the positive electrode.

Figure 4 indicates that the Al//GPE//graphite battery also possesses the advantages of flexibility, mitigated moisture sensitivity, and alleviated leakage corrosion. The Al//GPE//graphite battery is charged to 2.45 V at a constant density. As shown in Figure 4a–c, the open circuit voltage can keep above 2 V and lights up a red light emitting diode (LED) lamp when the Al//GPE//graphite battery is even under bent and folded states, indicating outstanding flexibility of the Al//GPE//graphite battery. When the battery is partially cut off, the remaining portion can still light up the red LED lamp even after being folded (Figure 4d–f). There is no liquid electrolyte leakage from the inside of the cutting battery, which is due to the encapsulation of ionic liquid by the polyamide matrix and benefits to mitigate both the moisture sensitivity and the leakage corrosion of ionic liquid. After being exposed to the air for 10 min, GPE and the $\text{AlCl}_3/\text{Et}_3\text{NHCl}$ ($r = 1.7$) IL are used to assemble the Al//graphite batteries. As shown in Figure S9, the Al//graphite battery using the exposed $\text{AlCl}_3/\text{Et}_3\text{NHCl}$ ($r = 1.7$) IL electrolyte displays no capacity, which is because the electrochemical activity is lost for the $\text{AlCl}_3/\text{Et}_3\text{NHCl}$ ($r = 1.7$) IL after being exposed to air for 10 min (Figure S4). In contrast, the Al//graphite battery using the exposed GPE electrolyte still could display a capacity of $\sim 60\text{ mA g}^{-1}$ for 100 cycles.

We also use coin cells to assemble the Al//graphite batteries. The Al//graphite batteries using the GPE electrolyte could be cycled well (Figure S10a). However, the Al//graphite battery using the $\text{AlCl}_3/\text{Et}_3\text{NHCl}$ ($r = 1.7$) IL electrolyte could not work after a couple of cycles as shown in Figure S10b. This is

because the coin cell shells (stainless steel) are corroded (Figure S11 (right)). For the GPE electrolyte, the polymer matrix encapsulates the corrosive $\text{AlCl}_3/\text{Et}_3\text{NHCl}$ ($r = 1.7$) IL, resulting in depressed leakage corrosion (Figure S11 (left)).

4. CONCLUSIONS

A polyamide based gel polymer electrolyte with a low cost $\text{AlCl}_3/\text{Et}_3\text{NHCl}$ ionic liquid as a plasticizer was prepared through a facile process. The gel polymer electrolyte is characterized by easy preparation, alleviated leakage corrosion, and reduced moisture sensitivity features. The quasi solid state Al//graphite batteries assembled with the gel polymer electrolyte deliver considerable rate capability and excellent cycling performance. This work would benefit the practical applications of aluminum ion batteries.

■ AUTHOR INFORMATION

Corresponding Author

Huiping Du – College of Electronic Engineering and Automation, Shandong University of Science and Technology, Qingdao 266590, China; [orcid.org/0000 0001 8219 5603](https://orcid.org/0000-0001-8219-5603); Email: duhp@sdust.edu.cn

Authors

Zhidong Liu – College of Electronic Engineering and Automation, Shandong University of Science and Technology, Qingdao 266590, China

Xiaohang Wang – College of Electronic Engineering and Automation, Shandong University of Science and Technology, Qingdao 266590, China

Zhiyuan Liu – College of Electronic Engineering and Automation, Shandong University of Science and Technology, Qingdao 266590, China

Shuqing Zhang – College of Electronic Engineering and Automation, Shandong University of Science and Technology, Qingdao 266590, China

Zichuan Lv – College of Electronic Engineering and Automation, Shandong University of Science and Technology, Qingdao 266590, China

Yanyan Cui – Institute of Nanotechnology, Karlsruhe Institute of Technology (KIT), 76344 Eggenstein Leopoldshafen, Germany

Li Du – College of Electronic Engineering and Automation, Shandong University of Science and Technology, Qingdao 266590, China

Kaiming Li – College of Electronic Engineering and Automation, Shandong University of Science and Technology, Qingdao 266590, China

Guoxin Zhang – College of Electronic Engineering and Automation, Shandong University of Science and Technology, Qingdao 266590, China

Meng Chang Lin – College of Electronic Engineering and Automation, Shandong University of Science and Technology, Qingdao 266590, China

Notes

The authors declare no competing financial interest.

ACKNOWLEDGMENTS

This work was supported by the Qingdao Scientific and Technological Innovation High level Talents project: Aluminum ion power and energy storage battery (No. 17 2 1 1 zhc).

REFERENCES

- (1) Yang, Z.; Zhang, J.; Kintner Meyer, M. C. W.; Lu, X.; Choi, D.; Lemmon, J. P.; Liu, J. Electrochemical Energy Storage for Green Grid. *Chem. Rev.* **2011**, *111*, 3577–3613.
- (2) Tarascon, J. M.; Armand, M. Issues and Challenges Facing Rechargeable Lithium Batteries. *Nature* **2001**, *414*, 359–367.
- (3) Aricò, A. S.; Bruce, P.; Scrosati, B.; Tarascon, J. M.; van Schalkwijk, W. Nanostructured Materials for Advanced Energy Conversion and Storage Devices. *Nat. Mater.* **2005**, *4*, 366–377.
- (4) Yang, K.; Liu, Q.; Zheng, Y.; Yin, H.; Zhang, S.; Tang, Y. Locally Ordered Graphitized Carbon Cathodes for High Capacity Dual Ion Batteries. *Angew. Chem., Int. Ed.* **2021**, *60*, 6326–6332.
- (5) Xiang, L.; Ou, X.; Wang, X.; Zhou, Z.; Li, X.; Tang, Y. Highly Concentrated Electrolyte Towards Enhanced Energy Density and Cycling Life of Dual Ion Battery. *Angew. Chem., Int. Ed.* **2020**, *59*, 17924–17930.
- (6) Zhang, G.; Ou, X.; Cui, C.; Ma, J.; Yang, J.; Tang, Y. High Performance Cathode Based on Self Templated 3D Porous Micro crystalline Carbon with Improved Anion Adsorption and Intercalation. *Adv. Funct. Mater.* **2019**, *29*, No. 1806722.
- (7) Lin, M. C.; Gong, M.; Lu, B.; Wu, Y.; Wang, D.; Guan, M.; Angell, M.; Chen, C.; Yang, J.; Hwang, B.; Dai, H. An Ultrafast Rechargeable Aluminium Ion Battery. *Nature* **2015**, *520*, 324–328.
- (8) Kotobuki, M.; Lu, L.; Savilov, S.; Aldoshin, S. Poly(Vinylidene Fluoride) Based Al Ion Conductive Solid Polymer Electrolyte for Al Battery. *J. Electrochem. Soc.* **2017**, *164*, A3868–A3875.
- (9) Wu, Y.; Gong, M.; Lin, M. C.; Yuan, C.; Angell, M.; Huang, L.; Wang, D.; Zhang, X.; Yang, J.; Hwang, B.; Dai, H. 3D Graphitic Foams Derived from Chloroaluminate Anion Intercalation for Ultrafast Aluminum Ion Battery. *Adv. Mater.* **2016**, *28*, 9218.
- (10) Wang, D.; Wei, C.; Lin, M. C.; Pan, C.; Chou, H.; Chen, H.; Gong, M.; Wu, Y.; Yuan, C.; Angell, M.; Hsieh, Y.; Chen, Y.; Wen, C.; Chen, C.; Hwang, B.; Chen, C.; Dai, H. Advanced Rechargeable Aluminium Ion Battery with A High Quality Natural Graphite Cathode. *Nat. Commun.* **2017**, *8*, No. 14283.
- (11) Zhu, N.; Zhang, K.; Wu, F.; Bai, Y.; Wu, C. Ionic Liquid Based Electrolytes for Aluminum/Magnesium/Sodium Ion Batteries. *Energy Mater. Adv.* **2021**, *2021*, No. 9204217.
- (12) Li, C.; Patra, J.; Li, J.; Rath, P. C.; Lin, M.; Chang, J. A Novel Moisture Insensitive and Low Corrosivity Ionic Liquid Electrolyte for Rechargeable Aluminum Batteries. *Adv. Funct. Mater.* **2020**, *30*, No. 1909565.
- (13) Ambroz, F.; Macdonald, T. J.; Nann, T. Trends in Aluminium Based Intercalation Batteries. *Adv. Energy Mater.* **2017**, *7*, No. 1602093.
- (14) Zhou, J.; Yu, X.; Zhou, J.; Lu, B. Polyimide/Metal Organic Framework Hybrid for High Performance Al Organic Battery. *Energy Storage Mater.* **2020**, *31*, 58–63.
- (15) Wang, H.; Gu, S.; Bai, Y.; Chen, S.; Zhu, N.; Wu, C.; Wu, F. Anion Effects on Electrochemical Properties of Ionic Liquid Electro-

lytes for Rechargeable Aluminum Batteries. *J. Mater. Chem. A* **2015**, *3*, 22677.

(16) Zhang, E.; Wang, B.; Wang, J.; Ding, H.; Zhang, S.; Duan, H.; Yu, X.; Lu, B. Rapidly Synthesizing Interconnected Carbon Nanocage by Microwave Toward High Performance Aluminum Batteries. *Chem. Eng. J.* **2020**, *389*, No. 124407.

(17) Wang, H.; Gu, S.; Bai, Y.; Chen, S.; Wu, F.; Wu, C. High Voltage and Noncorrosive Ionic Liquid Electrolyte Used in Rechargeable Aluminum Battery. *ACS Appl. Mater. Interfaces* **2016**, *8*, 27444–27448.

(18) Angell, M.; Pan, C. J.; Rong, Y.; Yuan, C.; Lin, M. C.; Hwang, B.; Dai, H. High Coulombic Efficiency Aluminum Ion Battery Using An AlCl₃ Urea Ionic Liquid Analog Electrolyte. *Proc. Natl. Acad. Sci. U.S.A.* **2017**, *114*, 834–839.

(19) Gan, F.; Chen, K.; Li, N.; Wang, Y.; Shuai, Y.; He, X. Low Cost Ionic Liquid Electrolytes for Rechargeable Aluminum/Graphite Batteries. *Ionics* **2019**, *25*, 4243–4249.

(20) Ng, K. L.; Malik, M.; Buch, E.; Glossmann, T.; Hintennach, A.; Azimi, G. A Low Cost Rechargeable Aluminum/Natural Graphite Battery Utilizing Urea Based Ionic Liquid Analog. *Electrochim. Acta* **2019**, *327*, No. 135031.

(21) Tu, J.; Song, W.; Lei, H.; Yu, Z.; Chen, L.; Wang, M.; Jiao, S. Nonaqueous Rechargeable Aluminum Batteries: Progresses, Challenges, and Perspectives. *Chem. Rev.* **2021**, *121*, 4903–4961.

(22) Jiao, H.; Wang, C.; Tu, J.; Tian, D.; Jiao, S. A Rechargeable Al Ion Battery: Al/Molten AlCl₃ Urea/Graphite. *Chem. Commun.* **2017**, *53*, 2331–2334.

(23) Song, Y.; Jiao, S.; Tu, J.; Wang, J.; Liu, Y.; Jiao, H.; Mao, X.; Guo, Z.; Fray, D. J. A Long Life Rechargeable Al Ion Battery Based on Molten Salts. *J. Mater. Chem. A* **2017**, *5*, 1282–1291.

(24) Li, Z.; Li, X.; Zhang, W. A High Performance Graphite Graphite Dual Ion Battery Based on AlCl₃/NaCl Molten Salts. *J. Power Sources* **2020**, *475*, No. 228628.

(25) Tu, J.; Wang, J.; Zhu, H.; Jiao, S. The Molten Chlorides for Aluminum Graphite Rechargeable Batteries. *J. Alloys Compd.* **2020**, *821*, No. 153285.

(26) Wang, J.; Tu, J.; Jiao, H.; Zhu, H. Nanosheet Stacked Flake Graphite for High Performance Al Storage in Inorganic Molten AlCl₃-NaCl Salt. *Int. J. Miner., Metall. Mater.* **2020**, *27*, 1711–1722.

(27) Xu, H.; Bai, T.; Chen, H.; Guo, F.; Xi, J.; Huang, T.; Cai, S.; Chu, X.; Ling, J.; Gao, W.; Xu, Z.; Gao, C. Low Cost AlCl₃/Et₃NHCl Electrolyte for High Performance Aluminum Ion Battery. *Energy Storage Mater.* **2019**, *17*, 38–45.

(28) Sun, X. G.; Fang, Y.; Jiang, X.; Yoshii, K.; Tsuda, T.; Dai, S. Polymer Gel Electrolytes for Application in Aluminum Deposition and Rechargeable Aluminum Ion Batteries. *Chem. Commun.* **2016**, *52*, 292–295.

(29) Yu, Z.; Jiao, S.; Li, S.; Chen, X.; Song, W. L.; Teng, T.; Tu, J.; Chen, H. S.; Zhang, G.; Fang, D. N. Flexible Stable Solid State Al Ion Batteries. *Adv. Funct. Mater.* **2019**, *29*, No. 1806799.

(30) Yu, Z.; Jiao, S.; Tu, J.; Song, W. L.; Lei, H.; Jiao, H.; Chen, H.; Fang, D. Gel Electrolytes with A Wide Potential Window for High Rate Al Ion Batteries. *J. Mater. Chem. A* **2019**, *7*, 20348–20356.

(31) Zhu, G.; Angell, M.; Pan, C. J.; Lin, M. C.; Chen, H.; Huang, C. J.; Lin, J.; Achazi, A. J.; Kaghazchi, P.; Hwang, B. J.; Dai, H. Rechargeable Aluminum Batteries: Effects of Cations in Ionic Liquid Electrolytes. *RSC Adv.* **2019**, *9*, 11322–11330.

(32) Das, S. K.; Mahapatra, S.; Lahan, H. Aluminium Ion Batteries: Developments and Challenges. *J. Mater. Chem. A* **2017**, *5*, 6347–6367.

(33) Porubská, M.; Szollos, O.; Konova, A.; Janigova, I.; Jaskova, M.; Jomova, K.; Chodak, I. FTIR Spectroscopy Study of Polyamide 6 Irradiated by Electron and Proton Beams. *Polym. Degrad. Stab.* **2012**, *97*, 523–531.

(34) Pockett, P. Crystallinity in Linear Polyamides: A Study Using Melt Blending with Small Molecule Diluents. Doctor of Philosophy Thesis, University of South Australia, 2004.

(35) Socrates, G. *Infrared and Raman Characteristic Group Frequencies: Tables and Charts*, 3rd ed.; John Wiley & Sons: Chichester, 2004; p 349.

(36) Roberts, M. F.; Samson, A. J. Site Specific Reversible Scission of Hydrogen Bonds in Polymers. An Investigation of Polyamides and Their Lewis Acid Base Complexes by Infrared Spectroscopy. *Macromolecules* **1991**, *24*, 3142–3146.

(37) Zhang, Z.; Huang, Y.; Gao, H.; Li, C.; Hang, J.; Liu, P. MOF Derived Multifunctional Filler Reinforced Polymer Electrolyte for Solid State Lithium Batteries. *J. Energy Chem.* **2021**, *60*, 259–271.

(38) Chen, H.; Xu, H. Y.; Wang, S. Y.; Huang, T. Q.; Xi, J. B.; Cai, S. Y.; Guo, F.; Xu, Z.; Gao, W. W.; Gao, C. Ultrafast All Climate Aluminum Graphene Battery with Quarter Million Cycle Life. *Sci. Adv.* **2017**, *3*, No. eaao7233.

(39) Chen, L.; Li, N.; Shi, H.; Zhang, Y.; Song, W.; Jiao, S.; Chen, H.; Fang, D. Stable Wide Temperature and Low Volume Expansion Al Batteries: Integrating Few Layer Graphene With Multifunctional Cobalt Boride Nanocluster as Positive Electrode. *Nano Res.* **2020**, *13*, 419–429.

(40) Liu, Z.; Wang, J.; Ding, H.; Chen, S.; Yu, X.; Lu, B. Carbon Nanoscrolls for Aluminum Battery. *ACS Nano* **2018**, *12*, 8456–8466.

(41) Chen, H.; Guo, F.; Liu, Y.; Huang, T.; Zheng, B.; Ananth, N.; Xu, Z.; Gao, W.; Gao, C. A Defect Free Principle for Advanced Graphene Cathode of Aluminum Ion Battery. *Adv. Mater.* **2017**, *29*, No. 1605958.

(42) Elia, G. A.; Kyeremateng, N. A.; Marquardt, K.; Hahn, R. An Aluminum/Graphite Battery with Ultra High Rate Capability. *Batteries Supercaps* **2019**, *2*, 83–90.

(43) Pan, C.; Yuan, C.; Zhu, G.; Zhang, Q.; Huang, C.; Lin, M. C.; Angell, M.; Hwang, B.; Kaghadzchi, P.; Dai, H. An Operando X ray Diffraction Study of Chloroaluminate Anion Graphite Intercalation in Aluminum Batteries. *Proc. Natl. Acad. Sci. U.S.A.* **2018**, *115*, 5670–5675.

(44) Schmuelling, G.; Placke, T.; Kloepsch, R.; Fromm, O.; Meyer, H. W.; Passerini, S.; Winter, M. X ray Diffraction Studies of The Electrochemical Intercalation of Bis(trifluoromethanesulfonyl)imide Anions into Graphite for Dual Ion Cells. *J. Power Sources* **2013**, *239*, 563–571.

(45) Dong, X.; Xu, H.; Chen, H.; Wang, L.; Wang, J.; Fang, W.; Chen, C.; Salman, M.; Xu, Z.; Gao, C. Commercial Expanded Graphite as High Performance Cathode for Low Cost Aluminum Ion Battery. *Carbon* **2019**, *148*, 134–140.

(46) Childress, A. S.; Parajuli, P.; Zhu, J.; Podila, R.; Rao, A. M. A Raman Spectroscopic Study of Graphene Cathodes in High Performance Aluminum Ion Batteries. *Nano Energy* **2017**, *39*, 69–76.

(47) Liu, C.; Liu, Z.; Niu, H.; Wang, C.; Wang, Z.; Gao, B.; Liu, J.; Taylor, M. Preparation and In Situ Raman Characterization of Binder Free u GF@CFC Cathode for Rechargeable Aluminum Ion Battery. *MethodsX* **2019**, *6*, 2374–2383.